Draft copy of paper submitted to IMechE, Part J, Journal of Tribology

THE WEAR EFFECTS AND MECHANISMS OF SOOT CONTAMINATED AUTOMOTIVE LUBRICANTS

D.A. GREEN*, R. LEWIS, R.S. DWYER-JOYCE

Department of Mechanical Engineering, The University of Sheffield, Mappin Street, Sheffield, S1 3JD

*Corresponding author

ABSTRACT

A study has been carried out to investigate the influence of soot contaminated automotive lubricants in the wear process of a simulated engine valve train contact. Previous research on this topic has been mainly performed from a chemical point of view in fundamental studies, with insufficient relevance to real engine conditions i.e. load and geometry. This study investigates the conditions under which wear occurs through specimen testing. The objective of the work was to understand the wear mechanisms that occur within the contaminated contact zone, to help in future development of a predictive wear model to assist in the valve-train design process.

The effects of soot in lubricants have been tested using a reciprocating test-rig specifically designed for this application, where a steel disc is held in a bath of oil and a steel ball (replicating a valve train contact) is attached to a reciprocating arm. The materials, contact geometry and loading conditions are all related to specific conditions experienced within an engine's valve-train. The testing was carried out under various contact conditions, using carbon black as a soot simulant. Wear measurements were taken during the tests and wear scar morphology was studied.

The results have revealed how varying lubrication conditions changes the wear rate of engine components and determines the wear mechanism that dominates for specific situations.

KEYWORDS

Carbon Black; Contaminated Lubricant; Soot; Valve Train; Engine Wear; Wear Modelling; Wear Map.

NOTATION

a	assumed radius of contact (m)	p_0	maximum contact pressure (N/m^2)
d	average wear scar depth (m)	p_m	mean contact pressure (N/m^2)
D	ball diameter (m)	P	applied load to contact (N)
E^*	reduced Young's modulus (N/m^2)	r	half spherical cap radius of wear scar (m)
H	hardness of wearing material (N/m^2)	R	ball radius (m)
K	dimensionless wear coefficient	V	volume of wear scar (m^3)
L	total sliding distance during wear test (m)		

1 INTRODUCTION

As internal combustion engine technology advances due to demands for improved fuel economy and performance, and lower oil consumption the many component contacts within an engine are operating under higher loads with thinner oil films to provide lubrication. This combined with the desire for increased service and oil drain intervals means that more wear problems are arising, which engine manufacturers are having to address as a matter of urgency so that their engines can meet all these requirements. There is currently a lack of wear models for lubricated engine components, leaving the understanding of the problem at a basic level that cannot be applied by engine designers. As part of a long term approach, wear models and design tools for engine components are required to increase understanding and reduce wear. The work detailed in this paper is part of a wider project to develop such models and tools for application by industry.

One major problem in the wear of engine components is due to soot that contaminates the lubricant. Soot is a microscopic carbonaceous particle, which is a product of incomplete combustion of hydrocarbons (in this case diesel fuel). Soot particles are more prevalent in diesel engines than gasoline engines due to the differences in the combustion mechanisms **[1]**.

In a diesel engine 29% of the soot produced reaches the atmosphere **[2]**. Of the soot that is retained in the engine (mainly in the lubricant), 3% is attributable to blow-by gases, the remainder results from piston rings scraping away soot deposits in the cylinder, which then end up in the sump **[3]**.

Soot particles are considered harmful, and as such emissions to the atmosphere are undesirable. A number of strategies are being employed to reduce these emissions such as; improving control over the in-cylinder charge condition, the fuel injection system and exhaust gas recirculation (EGR). EGR involves returning a proportion of the exhaust gas to the air intake. This results in a reduction in harmful NO_x emissions by reducing the peak burning temperature **[1]**. EGR, however, leads to a marked increase in particulate matter, including soot, remaining within the engine. If higher EGR ratios are introduced to combat emissions, there is an even greater need to understand how high levels of soot will affect wear.

Soot contamination has been shown to promote greater wear during engine tests with increasing levels of EGR **[3,4]** (see figure 1) and this has been replicated in simple specimen tests (such as the four-ball test method) **[5-7]**. However, there is still great uncertainty as to the mechanism of wear and the amount of wear that is produced and how this may relate to different contact geometries and motions and engine operating conditions. It has also not been determined what amount of soot a contact can tolerate.

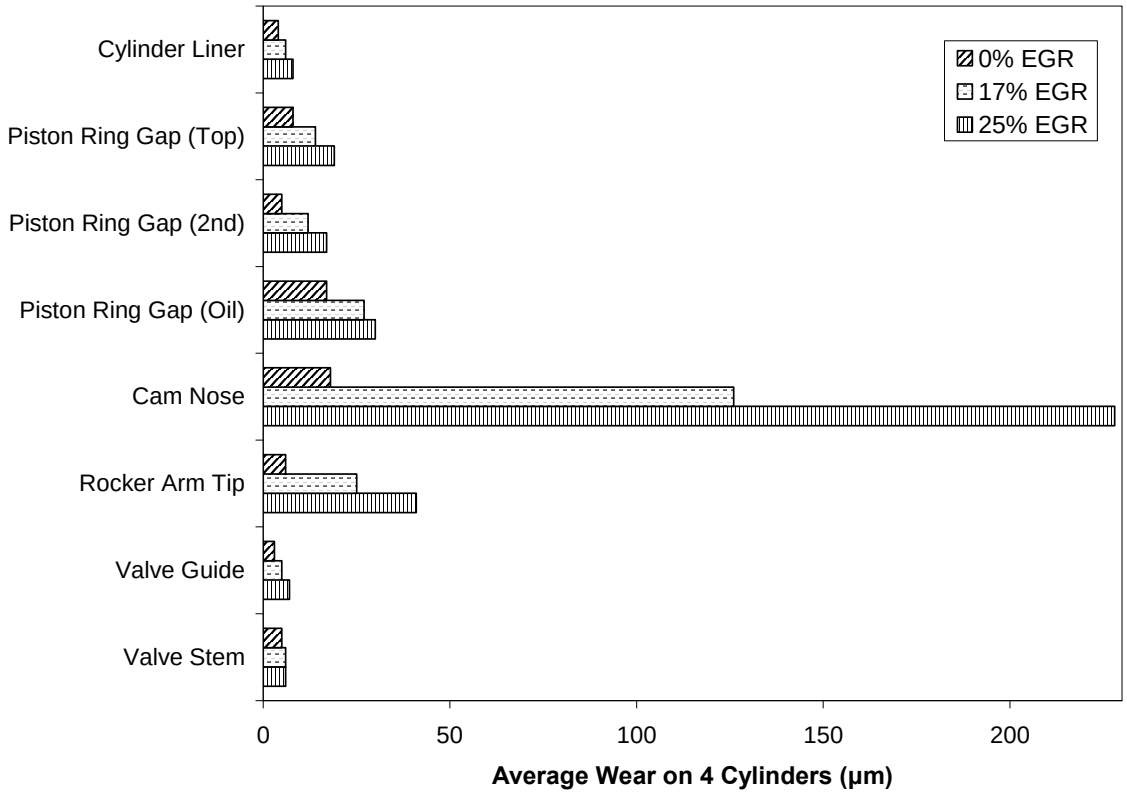

Figure 1. A reproduction of 4D55T/C Engine Wear Data **[4]** Showing Relative Component Wear Levels.

The aim of this work was to analyse a valve train component contact that is susceptible to soot induced wear to determine the contact conditions and motion and the lubrication regime and to design a specimen test to replicate these as closely as possible to allow tests to be carried out to identify changes in wear mechanism as soot concentration was varied as well as investigate the effect of varying temperature and sliding velocity (and hence lubricant film thickness).

2 BACKGROUND – SOOT WEAR THEORIES

As mentioned above, previous work investigating soot contamination of engines has been performed using engine testing and specimen testing, using standard approaches such as the four-ball method. Each of these techniques has their own advantages and disadvantages. With engine testing exact operating and environmental conditions are achieved, however, there is little control over variables as a result isolation of wear mechanisms is difficult as is determination of the wear magnitude. More control can be achieved with specimen tests, however, using simplified geometries means that soot entrainment is not realistically simulated.

The specimen testing carried out has led to three different wear mechanisms being proposed. Rounds **[5]**, postulated that chemical adsorption of the anti-wear components in the lubricant by the soot reduced the lubricant's ability to protect the surfaces. Other researchers have suggested that soot wear could occur due to starvation of lubricant in the contact. This is where soot agglomerates to dimensions greater that the oil film thickness and blocks lubricant entry to the contact **[8]**. The final mechanism proposed suggests that wear of the surfaces occurs by three body abrasion, where the soot acts as the third body. As agglomerates soot is

reasonably soft, but as individual particles, soot is thought to be hard enough to wear metal surfaces **[9]**. There is little work where actual component contacts at realistic operating conditions have been used to verify these theories.

To obtain a true understanding of engine component wear a combination of the above two testing methods is required, where actual engine contacts are investigated in specimen and individual component tests.

Individual or primary soot particles from diesel combustion have been measured to be approximately 40nm **[10]**. Due to soot's colloidal properties the particles agglomerate up to a maximum of approximately 500nm, with a mean soot agglomerate size of 200nm. Carbon black has been found to be an ideal soot surrogate as it very closely matches the properties of combustion soot and has been used extensively in specimen tests carried out to study soot wear.

Areas within the engine that have been shown to exhibit the greatest level of wear are in the valve train **[4]**. The cam nose was shown to have the greatest wear followed by the contacts on the rocker arm, see figure 1. Other valve train components with noticeable wear included the valve guides and stems. The contact between the cylinder wall/liner and the piston rings has also been highlighted as an area within engine to be highly susceptible to wear. All of these contacts exhibit reciprocating motion, with the exception of the cam nose which is a rolling/sliding motion. The rocker arm reciprocating contact has the simplest conditions to replicate in laboratory component tests.

3 SOOT WEAR OF THE ELEPHANT'S FOOT - CASE STUDY

An example of a rocker arm reciprocating contact is that of the elephant's foot to valve tip contact. A schematic diagram of the contact's reciprocating movement is shown in figure 2. This component has previously been shown to be susceptible to wear as shown by wear scar images in figure 3, comparing a new elephant's foot against a used one from a 2.4 litre, 16 valve diesel engine.

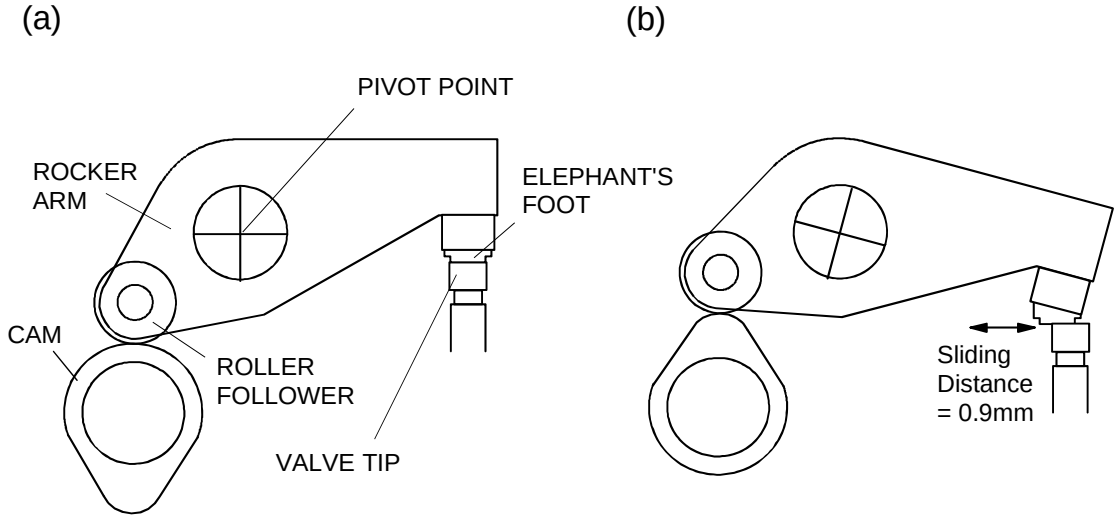

Figure 2. Rocker Arm Dimensions and Magnitude of Motion between (a) Valve Closed Position and (b) Valve Closed Position.

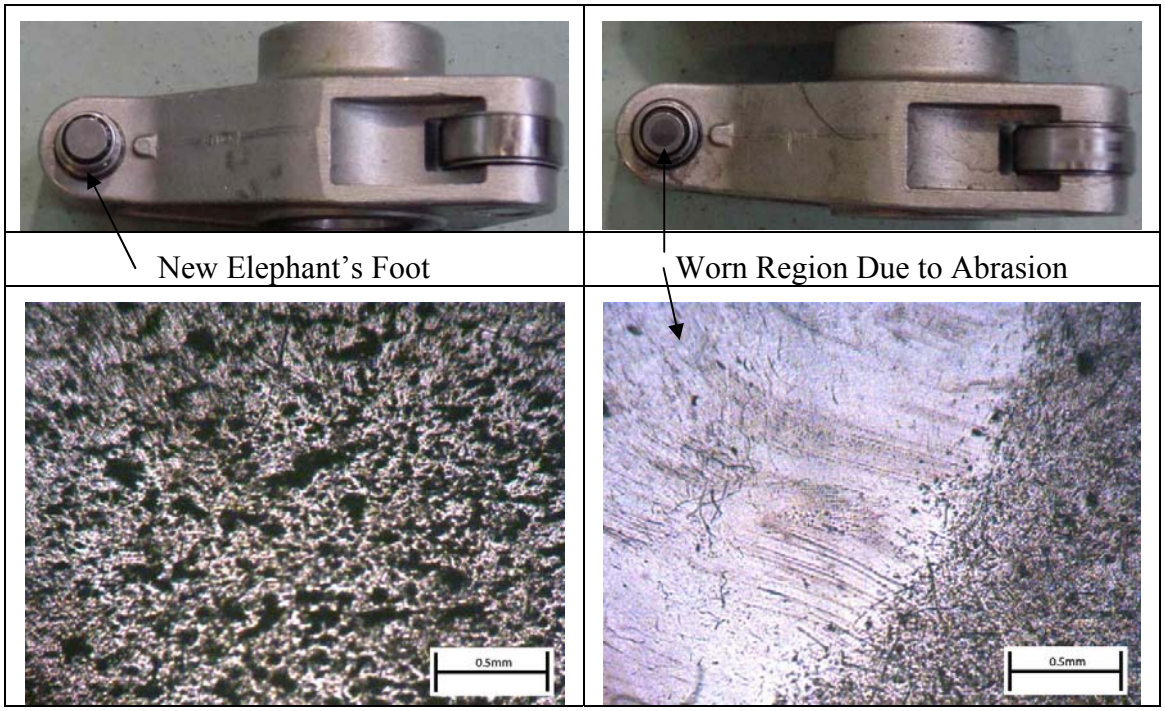

Figure 3. Comparison between the Surface of a New Elephant's Foot (left) and a Used Elephant's Foot (right).

Figure 3 clearly shows that considerable wear is visible on the surface of the elephant's foot that has been used in normal engine running conditions. The wear appears to be abrasive wear due to scratch marks in the direction of sliding marks on the surface of the component. Analysis reveals that through the wear process the rough surface becomes polished. Figure 3 also reveals that wear occurs only in the centre of the elephant's foot, this is because it is slightly radiused, probably to allow lubricating oil to be entrained into the contact. The effects of this wear could lead to changes in valve timing and lift.

The elephant's foot contact consists of two hard steel surfaces experiencing relatively high loads of up to 660N, reciprocating in a sinusoidal motion at an average speed of 0.0594m/s. The roughness of the surfaces of the elephant's foot (0.45μm) and the valve tip (0.175μm), combined with the experienced loads mean that the contact operates within the boundary lubrication regime.

To understand the levels of wear and the mechanisms that occur during use with soot contaminated lubricants a fundamental study is required. A simple approximation of the above contact is a ball on flat specimen test.

4. EXPERIMENTAL DETAILS

4.1 Experimental Simulation

The elephant's foot to valve tip contact was simulated by a ball-on-flat contact through Hertzian contact calculations **[11]**. Contact parameters were calculated assuming that the contact would be between a 5mm diameter steel ball against a flat steel counterface, with hardness's similar to the values of the elephant's feet and valve tips. The test contact conditions were chosen to simulate engine operating conditions, applicable to a range of component contacts to gain a fundamental understanding, rather than perform a direct comparison.

As the maximum contact pressure, p_0 of the actual contact is known, contact load required, P, could be obtained from:

$$P = \frac{2p_0\pi a^2}{3} \tag{1}$$

where the contact radius, a is:

$$a = \sqrt[3]{\frac{3PR}{4E*}} \tag{2}$$

The contact conditions and oil film thicknesses were calculated through Hertzian and EHD theory (see for example **[11]** and **[12]** respectively). The contact pressures and oil film thicknesses for the tests were selected to be as close as possible to the actual elephant's foot contact conditions.

It was decided to run tests at a sinusoidal mean sliding speed of 0.36m/s, and a lower speed of 0.18m/s to see if similar trends were obtained. These test sliding speeds are higher than those in the case study, to accelerate wear and to produce the required oil film thickness. The tested conditions are best compared through the theoretical film thicknesses; these are shown in Table 1. The film thicknesses are taken from the theoretical modelling detailed above. Table 1 highlights that increasing temperature and decreasing sliding speed have the combined effect of reducing oil film thickness. It is important to note that the conditions stated in table 1 all operate within the boundary lubrication regime.

		Oil used	Mean Soot Particle size (μm)	Soot Agglomerate size (μm)	Mean initial sample roughness (μm)	Minimum Film Thickness (μm)
25ºC	Ball on Flat (Full Speed)	Base Oil	0.2	0.5	0.42	0.075
25ºC	Ball on Flat (Half Speed)	Base Oil	0.2	0.5	0.42	0.055
100ºC	Ball on Flat (Full Speed)	Base Oil	0.2	0.5	0.42	0.02
100ºC	Ball on Flat (Half Speed)	Base Oil	0.2	0.5	0.42	0.01

Table 1. Comparison of Theoretical Film Thickness for Tested Conditions.

4.2 Test Apparatus

A universal high frequency reciprocating wear tester was used to carry out all of the wear tests. Figure 4 shows a simplified schematic diagram and Figure 5 shows a photograph of the wear tester. The tester holds the specimen balls in a clamp on the reciprocating arm and flat disc specimens in the heated base unit via another clamp. Prepared oil specimens (of approximately 2ml) are contained in the recessed zone with the flat disc specimens. The heated base is controlled by a programmable PID temperature controller. The reciprocator (LDS V201 vibrator) is controlled by a function generator. Friction measurements can be taken via a load cell located on the rig.

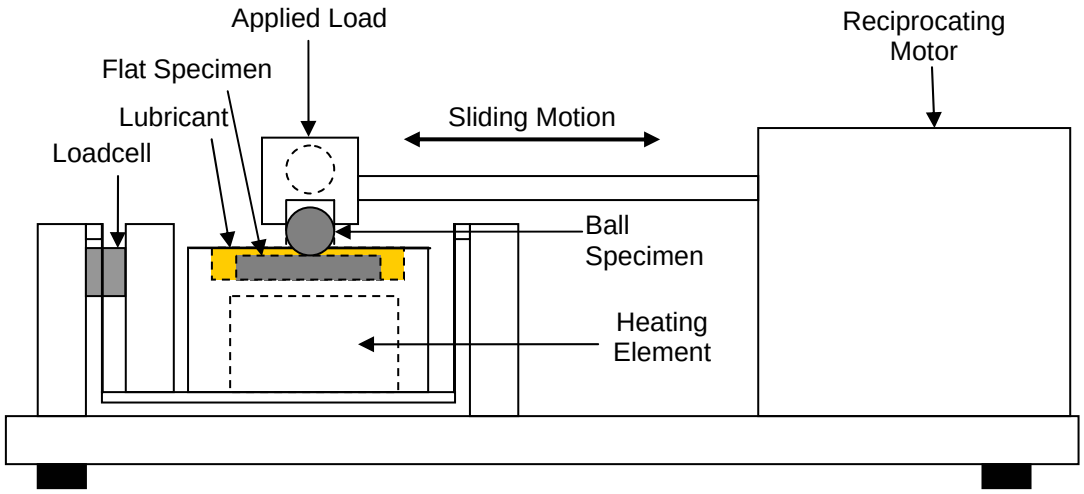

Figure 4. A Simplified Schematic Diagram of the Reciprocating Wear Tester.

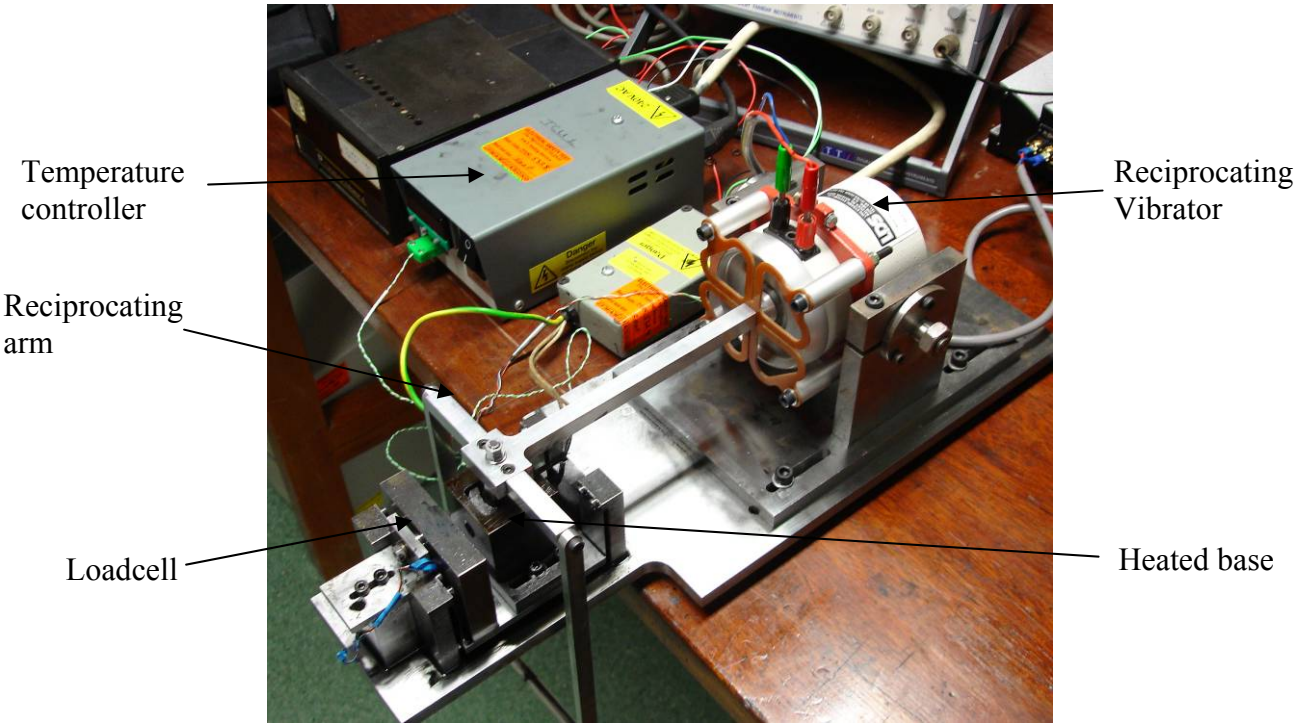

Figure 5. Universal Reciprocating Wear Tester.

4.3 Test Specimen Preparation

Details of the ball-on-flat specimens are shown in Table 2. The ball and flat test specimens were cleaned of any residue oxide layer or machining lubricant before the tests by washing in ethanol in an ultrasonic bath.

	Ball Specimen	Flat Specimen
Material	Chrome Steel EN31	EN24 Hardened & Tempered
Average Hardness (Hv)	600	400
Average Roughness (μm)	0.05	0.5
Young's Modulus, E (GPa)	210	210
Poisson's Ratio, ν	0.3	0.3
Diameter (mm)	5	18 (3mm thick)

Table 2. Details of ball on flat specimens.

4.4 Test Lubricant Preparation

The wear tests were performed with an automotive base oil as the test lubricant. This lubricant was used in tests on its own and mixed with varying amounts of carbon black and ashless dispersant (details of all components are shown in Table 3). No anti-wear additives were added to these base oil mixtures as this would affect the amount of wear measured, reduce the chemical independence of the testing and make the results specific to just one type of anti-wear additive. The mixing of ashless dispersant with the base oil is thought to have a negligible effect on the viscosity of the oil due to its low total weight content in the mixture and it will not add any anti-wear properties. The dispersant was purely mixed in to suspend the carbon black within the oil, as would occur in used formulated oil.

The mixed oils were prepared in 100g samples using a precision digital balance, which has a resolution of 0.01mg. The base oil mixtures contained a 4% (by weight) addition of ashless dispersant. The percentage of carbon black (by weight) required for the mixture was added (1 to5%), to produce a 100g sample.

The test lubricants were mixed using an ultrasonic bath for 20 minutes at 60ºC (the blending temperature of the dispersant with base oil is approximately 60ºC). An ultrasonic bath was used as the mixing device so as to reduce the chances of oil aeration; a spatula was used during the mixing process to ensure carbon black particles were being transported through the oil and did not reside on the bottom of the beaker.

Substance	Title	Description
Base oil	Shell HVI 60	Typical automotive base oil. Kinematic viscosity @ 40ºC = 24.83 cSt Dynamic viscosity (η_o) @ 40ºC = 0.019Ns/m^2 Kinematic viscosity @ 100ºC = 4.66 cSt Dynamic viscosity (η_o) @ 100ºC = 0.003 Ns/m^2 Density (approx.) = 750 kg/m^3
Ashless Dispersant	SAP 285	Lubricant dispersant for dispersing ash/soot.
Carbon Black	N/A	Acetylene black (AB) 50% compressed, 99.9+%

		(metals basis), mean particle diameter = 42nm.

Table 3. Test Lubricants and Components.

4.5 Test Procedure

The test equipment as described in Section 3.2 was used for each test. All tests were performed for 20 minutes. All full speed tests were performed at least three times, to ensure repeatability of results.

The oil temperature was the main parameter that was varied during the testing programme. The lubricant mixtures were tested at three different temperatures: room temperature (approximately 24ºC); engine working temperature (100ºC) and a ramped temperature profile of controlled linear heating from room temperature to 100ºC in 10 minutes and then held at 100ºC for the final 10 minutes. The test temperatures were to represent: cold working, normal engine working temperature and start-up conditions respectively. All constant test parameters are detailed in Table 4.

Reciprocating Distance (mm)	2 (amplitude)
Test duration (minutes)	20
Load (kg)	0.64 (including mass of arm)

Table 4. Constant Test Parameters.

Further tests were performed at half sliding speed to ensure the trends measured were consistent under various conditions.

To analyse how the wear varied with time, tests were also performed for 40 minutes with measurements taken every 10 minutes to measure how the wear scars developed, with an initial measurement taken after 3 minutes (to aid understanding of the early wear development). The tests were carried out at 25ºC and 100ºC with a 3% carbon black mixture.

4.6 Wear Measurement

The wear tests produced wear scars on the flat steel specimens and steel balls. The wear on the balls was negligible compared with that on the flat specimens and therefore not measured. The wear tests produced measurable grooves on the flat specimens. The length, l and width, w of a groove was measured using a digital camera and analysis software for accurate dimensioning. The wear depth of each groove was measured using a Mitutoyo Surftest Profilometer. As the depth varied along the length of the groove a number of depth measurements (transverse to the length of the groove) were taken. The experimental average depth, d was taken from these measurements. From this information the volume of a ‘perfect groove’ could be calculated, shown graphically in Figure 6.

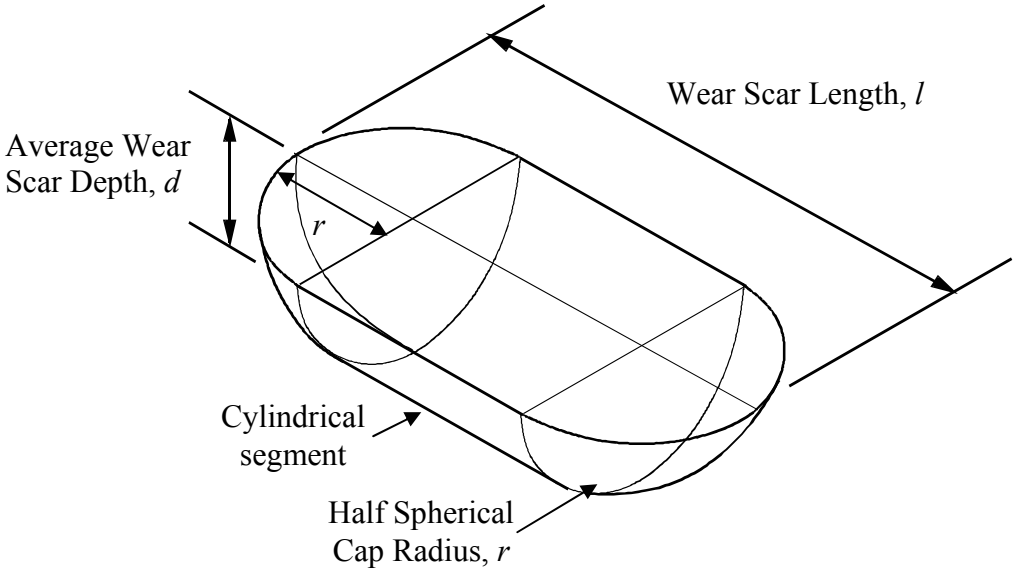

Figure 6. A 'Perfect Groove' Wear Scar

The 'perfect groove' consisted of a cylindrical segment and two half spherical caps at each end. Calculated using the following method, using a ball of 5mm diameter, *D* or 2.5mm radius, *R*:

Cylindrical Segment:

$$\text{Volume} = \left(R^2 \cos^{-1}\left(\frac{R-d}{R} \right) - (R-d)\sqrt{2Rd-d^2} \right)(l-2r) \tag{3}$$

Spherical Cap (whole cap):

$$\text{Volume} = \frac{1}{3}\pi d^2 (3R-d) \tag{4}$$

The total wear scar volume is the sum of the cylindrical segment and the spherical cap (whole cap).

5 RESULTS

5.1 Wear versus Carbon Black Content

The results of the main tests to evaluate the amount of wear produced from increasing level of carbon black contamination are shown in Figure 7. The amount of wear is represented as a percentage increase over the amount of wear produced by an identical wear test where the test lubricant is neat base oil with no contamination. These tests were performed at a sliding speed of 0.36m/s. Figure 7 presents results for the tests performed at 25ºC, with ramped heating (25-100 ºC ramp for 10 minutes, then held at 100ºC for a further 10 minutes), and at 100ºC.

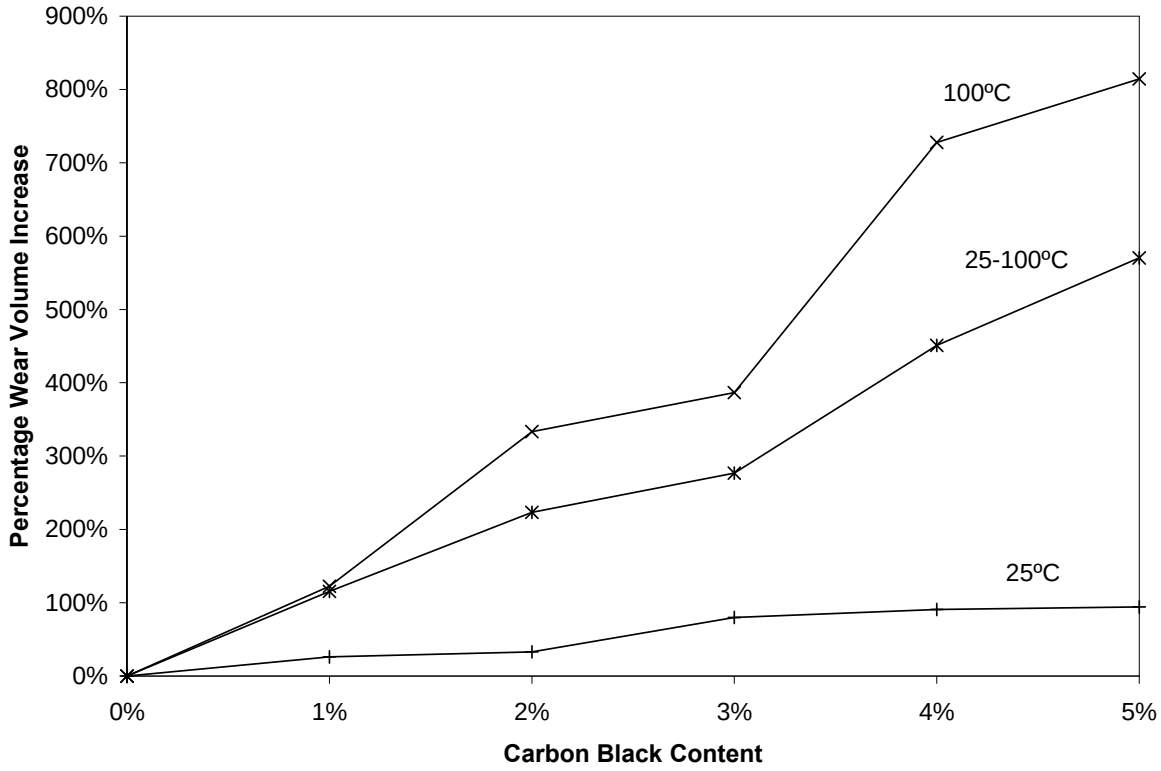

Figure 7. Results from Ball-on-Flat Testing Relative to 0% Carbon Black Content Tested at 25ºC, Ramped Heating and 100ºC (base oil at 0.36m/s).

The results in Figure 7 follow the expected trend of increased carbon black content and high test temperatures (due to their thin oil films) producing more wear. The wear levels measured for the ramped test are clearly between those of the 25ºC and 100ºC, as the ramped test involves conditions of both the 25ºC and 100ºC tests.

To ascertain whether the results measured in Figure 7 were true for a variety of contact conditions, further test were performed at a sliding speed of 0.18m/s (Figure 8). The results are again represented as a percentage increase over the amount of wear produced in a test using neat base oil.

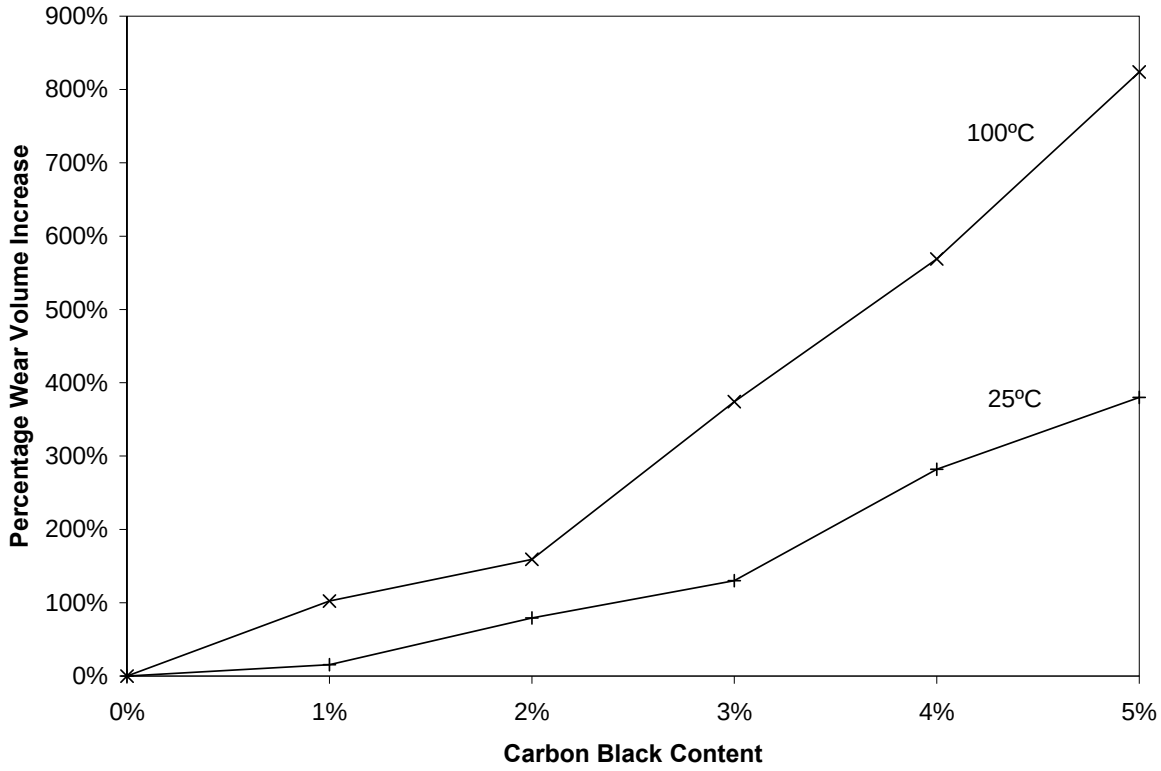

Figure 8. Results from Ball-on-Flat Testing Relative to 0% Carbon Black Content Tested at 25ºC and 100ºC (base oil at 0.18m/s).

All of the results follow a linear trend in wear volume with carbon black content up to 2% to 3% contamination level, at which point the gradient decreases (particularly so on the 0.36m/s results, shown in Figure 7), indicating a possible wear mechanism change. The gradient again changes after 4% contamination (for high temperature tests) indicating another wear mechanism change.

5.2 Wear Rate Results

The rate at which wear occurs during the tests is important as it can aid the understanding of the wear mechanisms. Wear rate tests using a sample of base oil mixed with 3% carbon black are shown in figure 9, the results are presented as increases in actual wear volume. The results show reasonably high wear rates during the first 5 to 10 minutes and by 10 minutes the majority of the wear has occurred. The results for the wear volume produced after 20 minutes of testing with neat base oil are displayed in figure 9 for comparison. It shows that carbon black contamination produces a greater wear volume, significantly so when the test temperature is 100ºC.

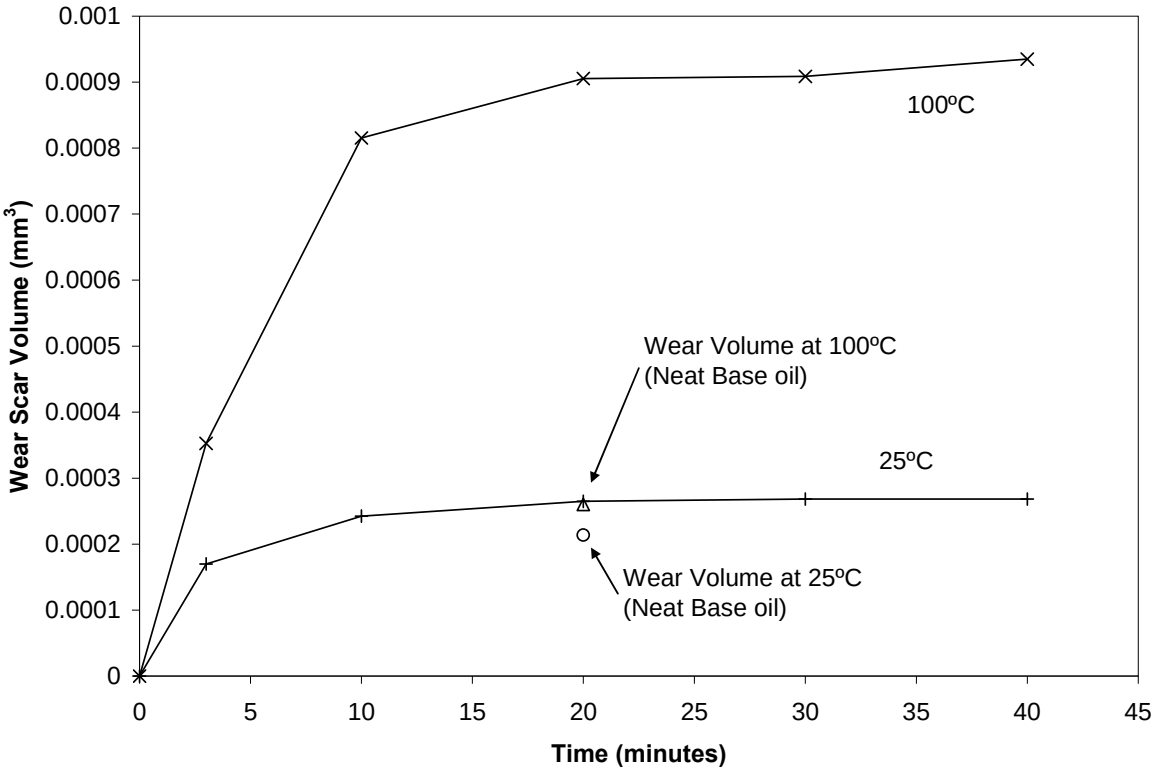

Figure 9. Results from Ball-on-Flat Wear Rate Testing with 3% Carbon Black Content Tested at 25ºC and 100ºC (base oil at 0.36m/s).

5.3 Friction Data

The friction measurements taken for all wear tests showed no appreciable change in friction coefficient with an increase in carbon black content. The tests produced friction coefficients of approximately 0.35 and 0.45 for 25ºC and 100ºC respectively. The friction coefficient for 100ºC is greater than that for the 25ºC tests as the oil film thickness for that temperature is lower by a factor of almost 4. The tests showed no variation of friction coefficient with soot content or time. Friction coefficient variation with carbon black (or soot) content has not previously been published as it appears to be extremely difficult to measure. Data has been published though, that shows friction coefficient is reduced when some soot is present in heavily used lubricating oil **[13]**; this is most likely to be related to the change in oil viscosity which is a factor of soot content and temperature. A more detailed study of these changes is required to investigate subtle variations in friction coefficient.

5.4 Morphology of Wear Scars

The wear scars presented in Figure 10 demonstrate how the characteristics of the wear produced varied with increasing carbon black content and change in temperature. The change in wear scar characteristics indicates possible changes in wear mechanisms.

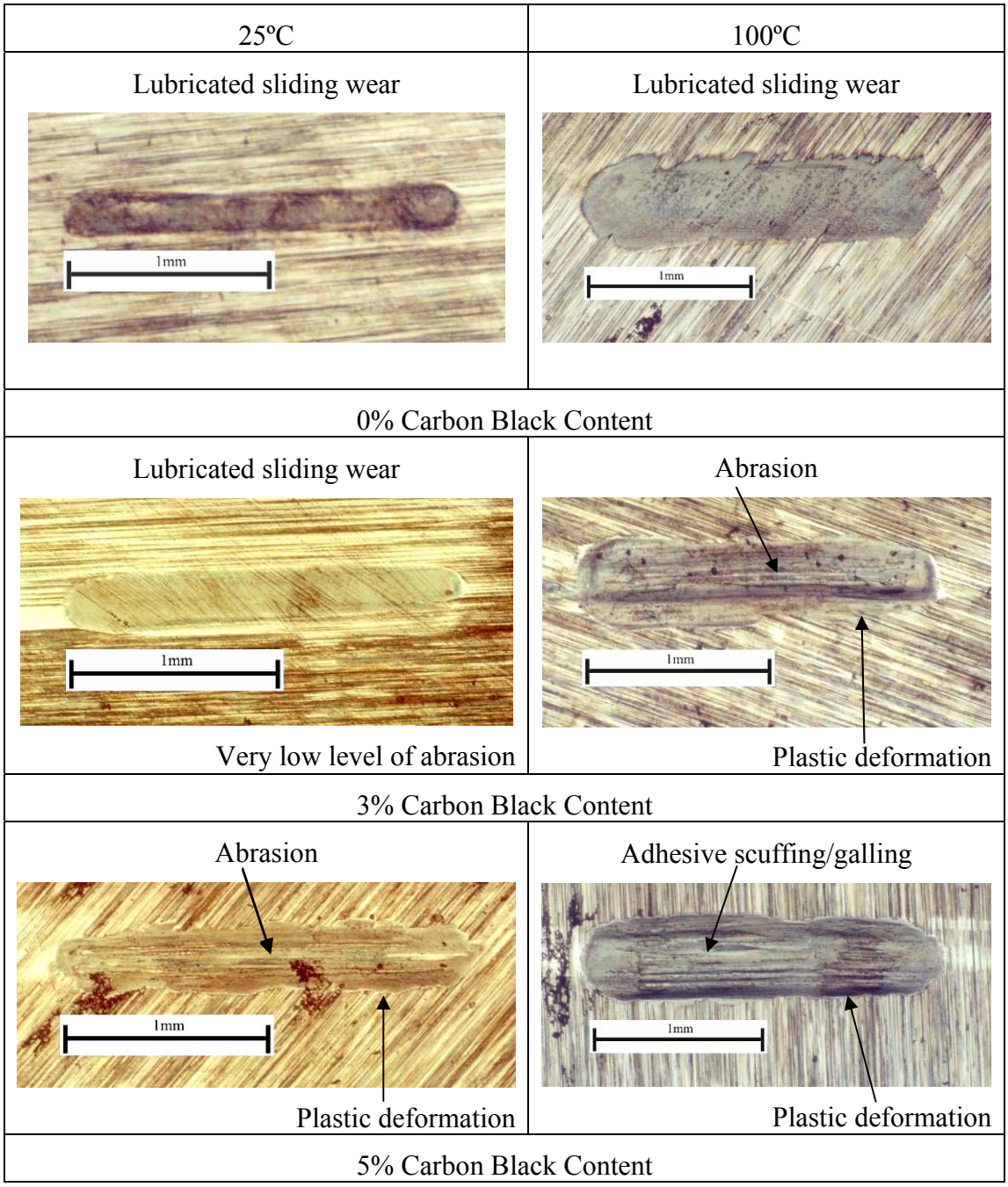

Figure 10. Images of Wear Scars for 1%, 3% and 5% at 25ºC and 100ºC.

Figure 10 clearly shows changes in the condition of the wear scar surface as the carbon black content of the test lubricant increases. At low levels of carbon black content the surface shows signs of mild lubricated metal-to-metal wear. The rough surfaces have been polished to a smooth finish and there are no scoring or abrasion marks. Evidence of machining marks still remain on the surfaces where low-level wear has occurred. As the carbon black content increases signs of abrasion in the direction of sliding and plastic deformation are evident from scoring marks and an uneven wear pattern around the circumference of the wear scar. The highest levels of carbon black content show increased levels of abrasion (as adhesive scuffing/galling wear) and plastic deformation indicating metal-to-metal contact, due to

possible starvation of lubricant from the contact. The visible evidence for lubricant starvation is the regions within the stroke showing signs of heavy metal-to-metal contact and some polishing wear.

6 DISCUSSION OF RESULTS

6.1 Reciprocating Wear Tests

The comparison of dimensions for the tested specimens show that higher sliding speeds produce thicker oil films and that higher temperatures produce thinner oil films. An understanding of these main points and how these dimensions compare to the various soot particle sizes explain why various test conditions produce more wear than others.

Figure 7 demonstrates that at both low and high temperatures, wear increases with increasing carbon black content. The 25°C wear tests show a very low increase in wear compared to the 100ºC tests. The 25ºC tests show that at 5% carbon black content the increase in wear volume is roughly 90% of the neat base oil tests. The 100ºC tests show that at 5% carbon black content the increase in wear volume is roughly 800% of the neat base oil tests. This dramatic increase in wear between the 25ºC and 100ºC tests is due to the oil film thickness decreasing by approximately a quarter, taking the film thickness much thinner than mean soot particle size.

The 25ºC results demonstrate a noticeable increase in wear between 2% and 3% contamination, and the 100ºC results demonstrate a noticeable increase in wear between 3% and 4% contamination; these increases may indicate a possible change in wear mechanism.

The ramped heating tests show increases in wear volume of a similar profile as the 100ºC tests. The increase in wear volume is less than the 100ºC tests, with an increase of just less than 600% of the neat base oil tests. This is because for the first 10 minutes of the tests the oil is operating in temperature regions where its thickness is relatively high compared to when it is operating at 100ºC, wear levels are then increased during the final 10 minutes of the tests when they are held at 100ºC. The wear levels for the ramped heating tests all appear to be approximately 70% of the 100ºC test results. Again there is an increase in wear between 3% and 4% contamination; indicating a possible change in wear mechanism.

The tests performed at half sliding speed (Figure 8) follow similar trends to those in figure 7. The wear measured is higher than those in figure 7, particularly so for the 25ºC tests, this is due to the oil film thickness reducing with the reduction in sliding speed. The wear for the 25ºC tests have increased dramatically because film thickness in this case is within the range of the carbon black agglomerates. For these test conditions the 25ºC tests show that at 5% carbon black content the increase in wear volume is nearly 400% of the neat base oil tests. The 100ºC tests show that at 5% carbon black content the increase in wear volume is over 800% of the neat base oil tests. Again there is an increase in wear between 2% and 4% contamination; indicating a possible change in wear mechanism.

6.2 Wear Rate Tests

The tests to measure the rate at which the wear occurs during tests showed that the majority of the wear occurs in the first 10 minutes – approximately 90%, shown in Figure 9. This follows the expected profile of a component experiencing ‘running-in’ and subsequent steady state wear, which is showing much higher levels of wear than would be seen with clean oil. The 100ºC tests exhibit approximately 4 times as much wear as the 25ºC tests – similar to the

levels measured in Figure 7. These results demonstrate that for such tests 20 minutes is a practical running time.

Figure 9 displays typical running-in of a component where lubricated metal-to-metal wear and abrasive wear normally dominates, producing a polished surface. After 20 minutes the results reaches threshold value where the two surfaces have become separated by the oil film. This threshold value will be a function of several factors, including: contact geometry, lubricant, temperature and contamination level. Figure 9 shows that carbon black contamination enhances this process, by performing a similar function to a grinding paste and increasing the wear level and therefore the component surface separation until a threshold (dependant on the contact conditions) has been reached.

6.3 Morphology of Wear Scars

With respect to Figure 10 it can be concluded that at both 25ºC and 100ºC the wear scars show typical lubricated metal-to-metal contact for the 0% carbon black content tests, but with the 100ºC case having greater wear. For the 3% carbon black content tests the 25ºC again shows signs of metal-to-metal contact, but with signs of a very low level of abrasion; the 100ºC case due to its thinner film thickness shows signs of abrasion and some plastic deformation. The 5% carbon black content test show at 25ºC signs of abrasion and some plastic deformation, the 100ºC tests show a great deal of abrasion and plastic deformation, and possible starvation of the lubricant from the contact.

6.4 Wear Mechanisms

From the above discussion, possible wear mechanisms can be proposed. These wear mechanisms are dependant on temperature (therefore oil film thickness) and carbon black content. For both low and high temperature (25ºC and 100ºC respectively) and low carbon black content (2% and below) there appears to be low levels of wear dominated by boundary lubricated metal to metal contact. This type of wear generally remains the case for higher carbon black contents (approximately 3%) and low temperatures, but with signs of low levels of abrasion. At 3% carbon black content and high temperatures wear is possibly occurring due to abrasion from entrained carbon black particles producing significant scratch marks, also showing signs of some plastic deformation. For the highest levels of carbon black content tested (5%) and low temperatures the wear mechanism appears to be similar to that of 3% carbon black and high temperatures, but at high temperatures another wear mechanism seems to be dominating. At both high carbon black content levels and temperature wear is possibly occurring due to high levels of abrasion and starvation due to particles blocking the contact region, dramatically reducing the flow of lubricant; again showing a large amount of plastic deformation. Component wear at such high contamination levels appears to be due to adhesive scuffing/galling wear.

The wear scars from the tests with the most heavily contaminated lubricant mixtures (figure 10), shows signs of all three wear mechanisms, where their formation is essentially dependant on the sliding speed within the stroke, see figure 11. At low sliding speeds (start of stroke), wear appears due to lubricated metal-to-metal contact as carbon black particles are not built-up around the contact (see point 1). At increasing sliding speeds the carbon black particles start to build-up around the contact, where the contaminant particles cause abrasive wear (see point 2). At the highest sliding speeds (mid stroke) carbon black particles have built-up enough before the contact to reduce lubricant flow into the contact zone and cause starvation and the associated metal-to-metal wear, shown by heavy scoring marks (see point 3) from

adhesive scuffing/galling wear. The above process occurs in reverse order during the second half of the stroke as the sliding speed decreases.

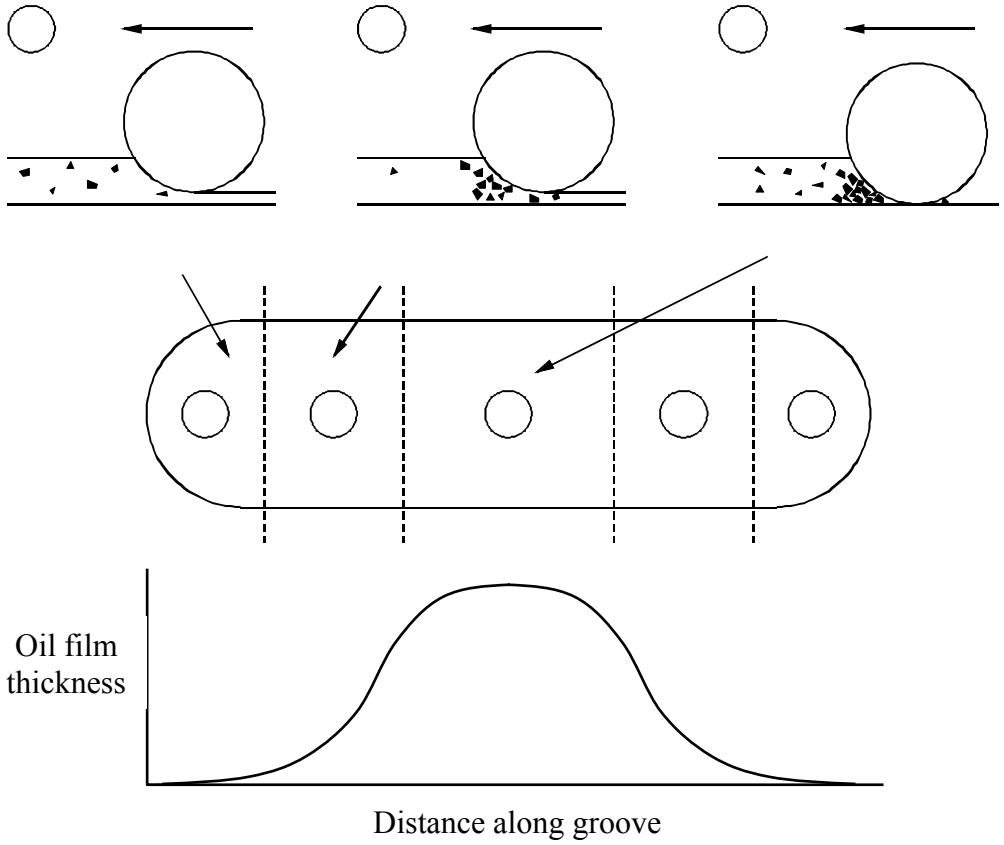

Figure 11. A Schematic of the Wear Mechanisms at a High Carbon Black Contamination Level.

These wear mechanisms are a direct effect of the carbon black content within the oil and cannot be attributed to additive depletion as no additives (except for ashless dispersant) were used in the tests. The amount of ashless dispersant available in the oil mixture for depletion will vary according to amount of carbon black in the mixture i.e. for high carbon black contents the ashless dispersant will mostly be depleted. The ashless dispersant gets depleted by adsorption on the carbon black to provide a steric stabilising layer. As the ashless dispersant additive is a low proportion of the test lubricant mixture, any possible effects are considered negligible. The measured wear correlated to carbon black concentration which tends to imply that wear is mainly due to an abrasive process, but with increased carbon black content contact starvation appears to dominate shown by a dramatic increase in wear.

6.5 Wear Modelling

Using the Archard wear equation **[14]**, wear coefficients can be calculated for each of the test conditions with the ball on flat testing, using the following dimensionless equation:

$$K = \frac{VH}{PL} \tag{5}$$

The wear coefficients are shown graphically in figure 12. For comparison the wear coefficient for an unlubricated ball on flat test at 25ºC is 9.6×10^{-5}. Wear coefficients are an extremely useful method of categorising wear for a particular situation into a standard format. Such wear coefficients can be applied to current wear models to increase the accuracy of wear predictions.

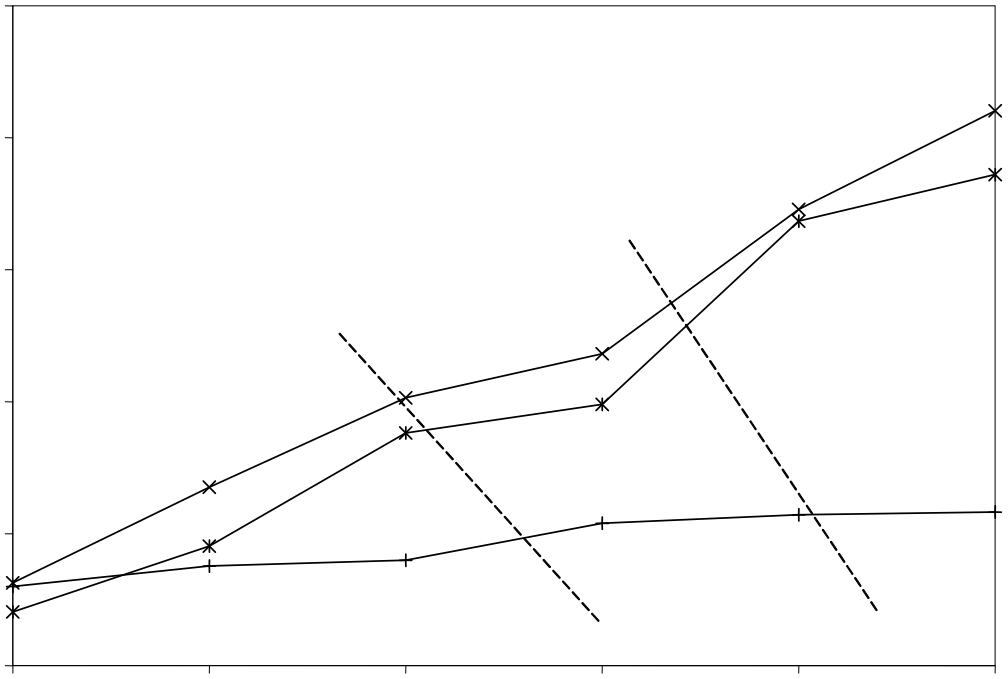

Figure 12. Wear Levels Plotted as Wear Coefficient against Carbon Black Content. Wear Mechanism Regimes are Indicated.

The coefficients detailed in figure 12 compare favourably with previously measured wear coefficients by Rabinowicz **[15]**. The results are within the region of excellent lubrication for identical metals and 3-body abrasive wear. The distinct regions of the wear mechanisms highlighted earlier are highlighted as three regions in figure 12, giving an indication of wear regimes.

7 CONCLUSIONS

This paper has detailed work to fully examine the contact and lubrication conditions of a simplified specimen test.

The following observations arose from the work:

- Increasing levels of carbon black content in base oil promote increased levels of component wear.
- Wear levels dramatically increase as temperature increases due reduced oil film thicknesses.
- For this kind of boundary lubrication contact, the results showed a series of wear mechanisms, with increasing carbon black content:

1. Lubricated metal to metal sliding wear. Lubricated metal to metal sliding contact conditions are generally evident below 2% carbon black content.
2. Abrasion due to the carbon black particles in the contact, occurring between 2% and 4% carbon black content.
3. Starvation of lubricant from the contact. The change between abrasion and starvation is thought to occur above approximately 4% carbon black content.

- The wear data measured has been shown as a wear map relating wear coefficient to carbon black content with the effect of temperature.

This work has confirmed the theories proposed by previous authors that soot contaminated lubricants will increase the wear of automotive components. Wear mechanisms have been proposed and presented as wear map. This work can be developed with testing of a variety of valve train components and used automotive lubricants.

8 REFERENCES

1 **Robert Bosch GmbH** *Automotive Handbook*, 1996, Fourth Edition, Bentley Publishers, Cambridge MA, USA.

2 **Daido, S., Kodama, Y., Inohara, T., Ohyama, N. and Sugiyama, T.** *Analysis of Soot Accumulation inside Diesel Engines*, 2000, JSAE Review, Vol. 21, pp303-308.

3 **Dennis, A.J., Garner, C.P., and Taylor, D.H.C.** *The Effect of EGR on Diesel Engine Wear*, 1999, SAE Paper No. 1999-01-0839.

4 **Nagai, I., Endo, H., Nakamura, H. and Yano, H.** *Soot and Valve Train Wear in Passenger Car Diesel Engines*, 1983, SAE Paper No. 831757.

5 **Rounds, F.G.** *Carbon: Cause of Diesel Engine Wear?*, 1977, SAE Paper No. 770829.

6 **Kim, C., Passut, C. A. and Zang, D. M.** *Relationships Among Oil Composition Combustion-Generated Soot, and Diesel Engine Valve Train Wear*, 1992, SAE 922199.

7 **Sato, H., Tokuoka, N., Yamamoto, H. and Sasaki, M.** *Study on Wear Mechanism by Soot Contamination in Engine Oil*, 1999, SAE Paper No. 1999-01-3573.

8 **Yoshida, K. and Sakurai, T.** *Some Aspects of Tribological Behaviour on Dispersed-Phase System*, 1998, Lubrication Engineering, Vol. 44, pp913-921.

9 **Gautam, M., Durbha, M., Chitoor, K., Jaraiedi, M., Mariwalla, N. and Ripple, D.** *Contribution of Soot Contaminated Oils to Wear*, 1998, SAE Paper No. 981406.

10 **Clague, A.D.H., Donnet, J.B., Wang, T.K. and Peng, J.C.M.** *A Comparison of Diesel Engine Soot with Carbon Black*, 1999, Carbon, Vol. 37, pp1553-1565.

11 **Williams, J.A.** *Engineering Tribology*, 1994, Oxford University Press.

12 **Hamrock, B.J., Schmid, S.R. and Jacobson, B.O.** *Fundamentals of Fluid Film Lubrication, 2nd Edition*, 2004, Marcel Dekker, Inc.

13 **Fujita, H. and Spikes, H.** *The influence of soot on lubricating films*, 2004, Proceedings of the 30th Leeds-Lyon Symposium on Tribology.

14 **Archard, J.F.** *Contact and Rubbing of Flat Surfaces*, 1953, Journal of Applied Physics, Vol. 24, No. 8, pp981-988.

15 Rabinowicz, E. *The Wear Coefficient – Magnitude, Scatter, Uses*, 1981, Transactions of the ASME, Vol. 103, pp188-194.